TRR
JOURNAL OF THE TRANSPORTATION RESEARCH BOARD

Infrastructure

Transportation Research Record
2019, Vol. 2673(6) 492–500

DOI: 10.1177/0361198119853544
journals.sagepub.com/home/trr
SAGE

Simple Method to Evaluate Strength and Relaxation Properties of Asphalt Binders at Low Temperature

Jhenyffer Matias De Oliveira[1], Tianhao Yan[1], Mugurel Turos[1], Debaroti Ghosh[2], Dave Van Deusen[2], and Mihai Marasteanu[1]

Abstract
Low temperature cracking represents the main distress in asphalt pavements built in cold regions. During the Strategic Highway Research Program (SHRP) two test methods were developed to investigate the low temperature behavior of asphalt binders: bending beam rheometer (BBR) and direct tension tester (DTT). In this research, a simple testing protocol developed to obtain failure properties of asphalt binders at low temperatures is used to characterize the behavior of five asphalt binders used in the construction of MnROAD test cells in 2016. It is shown that a combination of creep followed by strength testing provides a more complete picture of the low temperature properties of asphalt binders and can improve the selection process. Binders with similar creep and relaxation properties have significantly different failure properties. It is also demonstrated that BBR strength data is obtained under linear viscoelastic conditions for the entire duration of the test and that creep and strength data can be interconverted using linear viscoelasticity.

The characterization of asphalt binder at low temperatures is currently performed as part of the performance grade (PG) system developed during the Strategic Highway Research Program (SHRP) at the beginning of the 1990s (*1*). The PG system consists of two temperature limits; the first relates to the response of the binder at high service temperature and the second provides information on the low temperature behavior. Currently, low temperature properties of asphalt binders are evaluated using the bending beam rheometer (BBR) (*2*) and direct tension tester (DTT) (*3*). The BBR is used to perform low temperature creep tests for 240 s on beams of pressure aging vessel (PAV) aged asphalt binders conditioned at the desired temperature for 1 h. Creep stiffness, which is the inverse of creep compliance, and the slope of creep stiffness versus time curve on a double logarithmic scale, which can be related to relaxation of thermal stresses that build up at low temperatures, were selected as performance criteria. The DTT is used to perform uniaxial tension tests on a dog bone shaped specimen at a constant strain rate of 3%/min until failure. According to Dongré, the strain rate and strain limit were chosen based on practical considerations: shorten the test duration to less than 1 min and obtain limiting temperatures similar to limiting temperatures obtained from BBR creep data (*4*).

The high cost of DTT and complex sample preparation made the test less appealing to industry, and some agencies do not use the DTT to determine the PG of the binder. In addition, it was previously shown that DTT devices are not capable of maintaining a constant strain of 3%/min (*5*), which makes the experimental data difficult to interpret based on linear viscoelasticity concepts for research purposes.

The creep stiffness obtained with the current BBR can be related to thermal stress accumulation as temperature drops to negative values; however, without knowledge of failure properties, it is impossible to correctly predict the cracking resistance of these materials, especially for modified binders.

[1]University of Minnesota, Twin Cities, Minneapolis, MN
[2]Minnesota Department of Transportation, Maplewood, MN

Corresponding Author:
Address correspondence to Tianhao Yan: yan00004@umn.edu

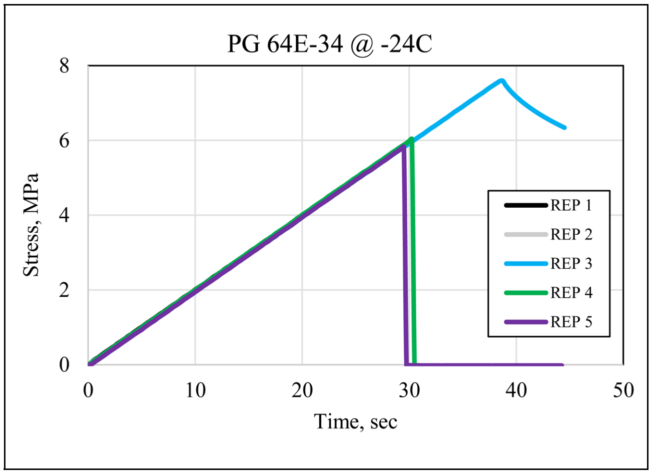

Figure 1. Loading rate for strength test performed at −24°C on Cell 23 asphalt binder.

Development of BBR Strength Testing Procedure

In previous work, the authors have proposed a new strength testing method using a modified BBR device, called BBR-Pro (*6*). In their investigation, the authors demonstrated that, by taking into account the size effect and the cooling medium effect, the DTT and the BBR strength testing methods result in strength values that are similar (*6, 7*). Note that, at the two PG test temperatures used in the analysis, the strength is equal to the peak stress.

By imposing constraints related to the duration of the test (1 min for practical reasons, similar to the criterion used for establishing the strain rate for DTT), and knowing that, based on hundreds of tests performed, the failure stress does not exceed 12MPa, a loading rate of 0.65 N/s was proposed for routine testing (*8*). The tests are performed at PGLT + 10°C and also at PGLT + 4°C, similar to current BBR and DTT specifications. PGLT stands for performance grade low temperature limit. The strength tests can be performed after a 240 s recovery period immediately after BBR creep testing, or they can be performed as a separate test on new binder specimens. The first method is much shorter and requires less asphalt binder, because the creep and strength tests are performed on the same beam of asphalt binder.

Unlike DTT experiments, in which the strain rate is not constant, in the BBR stress-controlled test the stress rate remains constant for the entire duration of the test. An example is shown in Figure 1.

This also means that, unlike DTT experiments, in which the stress–strain data could not be related to relaxation modulus because of changes in strain rate during the test, the BBR strength data can be related to creep compliance. This is demonstrated below.

In a test in which the stress is increased linearly starting from zero, the resulting strain will reflect the superposition of a series of retarded compliances (*9*). If $\dot{\sigma} = \mathrm{d}\sigma/\mathrm{d}t$ is the rate of stress increase, then

$$\varepsilon = \dot{\sigma} t J_g + \dot{\sigma} \int_0^t \int_{-\infty}^{\infty} L(\tau)(1 - e^{-u/\tau}) \mathrm{d} \ln \tau \mathrm{d}u + \frac{\dot{\sigma} t^2}{2\eta_o} \quad (1)$$

$$\varepsilon = \dot{\sigma} t J_g + \dot{\sigma} \int_{-\infty}^{\infty} L(\tau) \left[t - \tau \left(1 - e^{-t/\tau} \right) \right] \mathrm{d} \ln \tau + \frac{\dot{\sigma} t^2}{2\eta_o} \quad (2)$$

where
ε is the strain;
J_g is the glassy compliance;
$L(\tau)$ is the retardation spectrum;
τ is the retardation time; and
η_o is the Newtonian viscosity.

When the stress–strain curve under this condition is differentiated, the result is the creep compliance, $J(t)$:

$$\frac{\mathrm{d}\varepsilon}{\mathrm{d}\sigma} = (1/\dot{\sigma}) \frac{\mathrm{d}\varepsilon}{\mathrm{d}t} = J_g + \int_{-\infty}^{\infty} L \left(1 - e^{-t/\tau} \right) \mathrm{d} \ln \tau + t/\eta_o = J(t) \quad (3)$$

Therefore, if creep compliance is known, the variation of strain with stress is known for a constant loading rate test. If this loading rate is known, then the entire stress–strain curve can be determined.

Previously, the authors used a simple approximation to predict stress–strain curve, for a given loading rate, from creep compliance. First, assume that the BBR strength test is performed at a constant stress rate $\dot{\sigma}$. The stress at any time can be simply calculated as

$$\sigma(t) = \dot{\sigma}^* t \quad (4)$$

By making the assumption that the creep compliance $J(t)$ obtained in the creep test follows a power law of the stress in the strength test, it is possible to obtain

$$J(t) = a^* \{\sigma(t)\}^b \quad (5)$$

Coefficients a and b can be simply calculated by fitting Equation 5 to the creep compliance versus stress curve, for an assumed loading rate. The loading rate value is required to match the times for the creep compliance (obtained in the creep test) and the stress (in the strength test).

From Equation 5, the first derivative of the strain–stress curve is the creep compliance, $J(t)$, and, therefore, Equation 5 can be rewritten as

$$J(t) = \mathrm{d}\varepsilon(t)/\mathrm{d}\sigma(t) = a^* \{\sigma(t)\}^b \quad (6)$$

The strain can then be obtained as

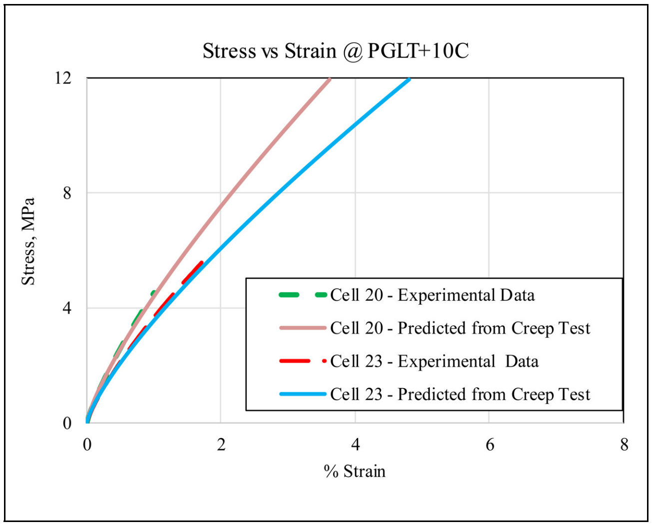

Figure 2. Predicted and experimentally determined stress–strain curves for two binders.

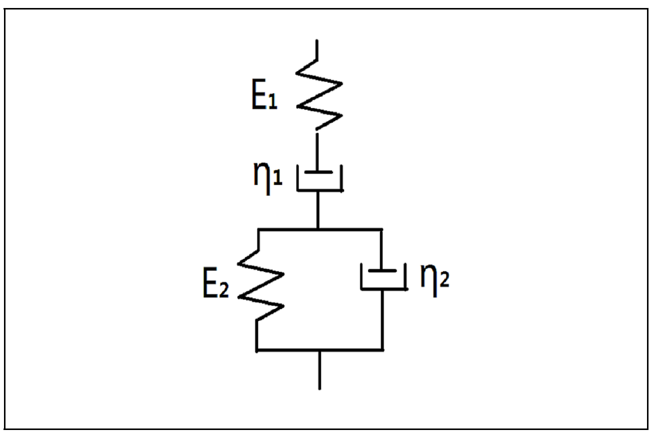

Figure 3. Burgers model.

$$\varepsilon(t) = \frac{a^*\{\sigma(t)\}^{b+1}}{b+1} + c \tag{7}$$

Constant c is zero as the plot starts in origin.

An example is presented in Figure 2.

An alternative method is to use the Burgers model commonly used to analyze the linear viscoelastic behavior of asphalt binders. The model is shown in Figure 3.

The expression for creep compliance is

$$J(t) = \frac{1}{E_1} + \frac{t}{\eta_1} + \frac{1}{E_2}\left(1 - e^{-\frac{tE_2}{\eta_2}}\right) \tag{8}$$

where E_1 and η_1 represent the linear spring constant (modulus) and the dashpot coefficient of viscosity of the Maxwell model, and E_2 and η_2 represent the linear spring constant (modulus) and the dashpot coefficient of viscosity of the Kelvin model, as shown in Figure 3.

The stress history for the creep and recovery test is written as

$$\sigma(t) = \begin{cases} \sigma_0 H(t) \\ \sigma_0 H(t) - \sigma_0 H(t - t_0) \end{cases} \tag{9}$$

where

$H(t)$ is the Heaviside step function;

σ_0 is the amplitude of the constant loading in the creep test; and

t_0 is the time when the creep test ends and the recovery test begins.

Based on the linear superposition principle of viscoelasticity, the corresponding deflection can be calculated as

$$\varepsilon(t) = \begin{cases} \sigma_0 J(t) & 0 < t < t_0 \\ \sigma_0 J(t) - \sigma_0 J(t - t_0) & t > t_0 \end{cases} \tag{10}$$

Substituting Equation 8 into Equation 10 obtains the strain history for creep and recovery.

When $0 < t < t_0$

$$\varepsilon(t) = \sigma_0\left(\frac{1}{E_1} + \frac{t}{\eta_1} + \frac{1}{E_2}\left(1 - e^{-\frac{tE_2}{\eta_2}}\right)\right) \tag{11}$$

When $t > t_0$

$$\varepsilon(t) = \sigma_0\left(\frac{t_0}{\eta_1} + \frac{1}{E_2} e^{-\frac{tE_2}{\eta_2}}\left(e^{\frac{t_0E_2}{\eta_2}} - 1\right)\right) \tag{12}$$

The loading expression for the strength test is

$$\sigma(t) = \alpha t \tag{13}$$

where α is the loading rate.

Based on linear viscoelasticity, strain history can be calculated as the following convolution:

$$\varepsilon(t) = \int_{-\infty}^{t} J(t - \xi)\dot{\sigma}(\xi)d\xi \tag{14}$$

Substituting Equation 13 into Equation 14 and changing the integration variable to $\zeta = t - \xi$ obtains

$$\varepsilon(t) = \alpha \int_0^{\infty} J(\zeta)d\zeta \tag{15}$$

Substituting Equation 8 into Equation 15 and integrating obtains the strain in the strength test:

$$\varepsilon(t) = \alpha\left(\frac{t}{E_1} + \frac{t^2}{2\eta_1} + \frac{1}{E_2}\left(t - \frac{\eta_2}{E_2}(1 - e^{-\frac{tE_2}{\eta_2}})\right)\right) \tag{16}$$

Equations 11, 12, and 16 represent the expressions for creep, recovery, and strength tests, respectively. These three equations can be used to predict stress–strain curves from creep and recovery experimental data.

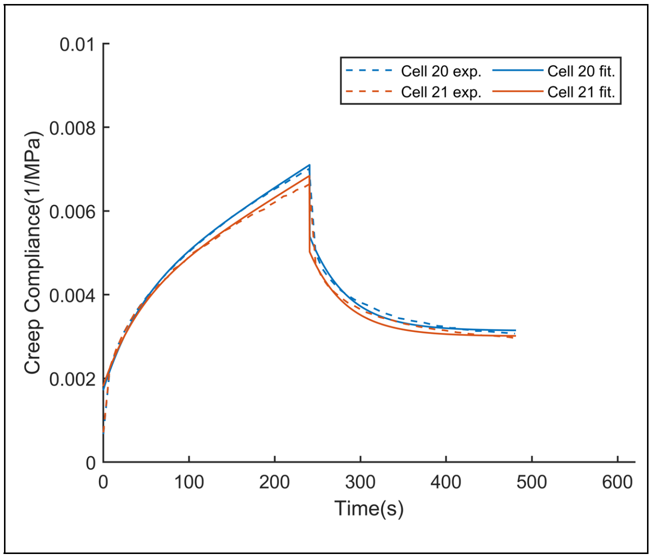

Figure 4. Using Burgers model to fit creep and recovery experimental data.

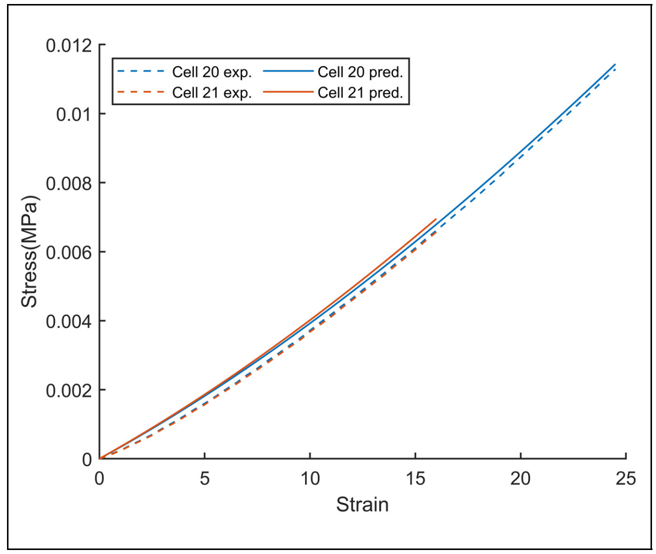

Figure 5. Using Burgers model to predict stress–strain curve.

Table 1. Burgers Model Parameters Result

Cell	E_1 (MPa)	η_1 (MPa*s)	E_2 (MPa)	η_2 (MPa*s)
Cell 20	582.45	76,792.34	442.89	19,492.50
Cell 21	550.45	80,030.50	494.07	21,253.46

An example is shown below for the binders used in Cells 20 and 21 at MnROAD. First, Equations 11 and 12 are used to fit the creep and recovery experimental data. As shown in Figure 4, the model fits very well with the experimental data.

The fitted model parameters are listed in Table 1.

The strain history for strength test can be predicted using Equation 16. As seen in Figure 5, the prediction matches very well the experimental data, which indicates one more time that the experimental strength data is obtained under linear viscoelastic condition in a constant stress test.

Experimental Laboratory Investigation

The simple procedure previously described was used to test five asphalt binders used in MnROAD Cells 16, 20, 21, 22, and 23 that were constructed in summer of 2016. All strength tests were performed after a 240 s recovery period following the creep test. Table 2 details the binders used as well as the mixtures prepared with the five binders. The first binder was a PG −22 and the remaining four binders were PG −34. The binder used in Cell 23 was highly modified. The binders in Cells 21 and 22 were the same; however, the binder in Cell 22 contained antistrip agent.

Both creep and strength properties were obtained using a BBR-Pro at PGLT + 10°C and PGLT + 4°C. All binders were PAV aged and all low temperature testing was performed in air. Six replicates were tested for each binder and each temperature. After the beams were conditioned for 1 h, a creep test was performed according to AASTHO T313. The beam was allowed to recover for 240 s and this was followed by a strength test at a constant loading rate of 0.65 N/s.

The experimental results and corresponding coefficients of variation (CoV) are shown in Figures 6 to 9. The results represent average values. For creep stiffness and *m*-value, the CoV values are less than 15% and 10%, respectively which indicates reasonable repeatability. For the BBR strength, the values are less than 25%, except for the binders from Cells 20 and 21 at the lowest test temperature of PGLT + 4°C.

The BBR strength results show a clear difference between the different types of asphalt binder. All binders pass the creep stiffness and *m*-value criteria at PGLT + 10°C (Figures 6 and 7). The binder from Cell 16 has similar stiffness value to the binder from Cell 23. However, the binder from Cell 16 has the lowest strength, whereas the binder from Cell 23 has the highest strength (Figure 8). This is also confirmed by average creep stiffness and stress–strain curves shown in Figures 10 and 11. A less obvious difference is observed for binders from Cells 20 and 21 that have almost the same creep stiffness and *m*-value, as shown in Figures 6 and 7. However, stress–strain curves in Figure 11 indicate that the binder from Cell 21 may perform better than the binder from Cell 22.

Table 2. Asphalt Binders Tested

Cell no.	Mix design	Binder	% RAP	% RAS	% Total AC	% Virgin AC	% Effective AC
16	SPWEB540L	PG 64S-22	20	5	5.3	3.2	4.6
20	SPWEB540A	PG 52S-34	30	0	5.3	3.5	4.6
21	SPWEB540C	PG 58H-34	20	0	5.4	4.2	4.6
22	SPWEB540C	PG 58H-34	20	0	5.7	4.2	4.5
23	SPWEB540I	PG 64E-34	15	0	5.2	4.2	4.5

Note: no. = number; RAP = reclaimed asphalt pavement; RAS = reclaimed asphalt shingles; AC = asphalt content.

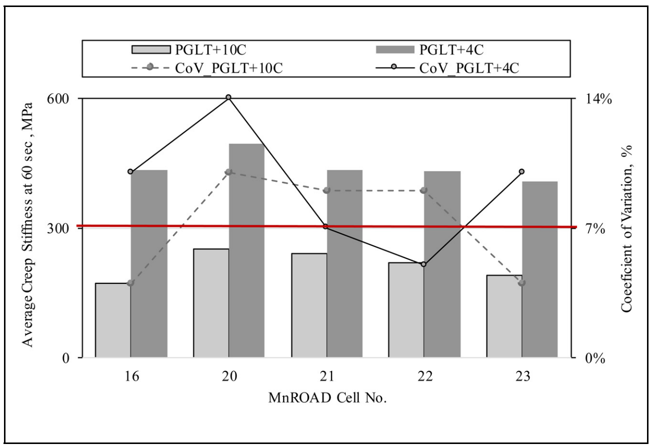

Figure 6. Creep stiffness at 60 s at PGLT + 10°C and PGLT + 4°C.

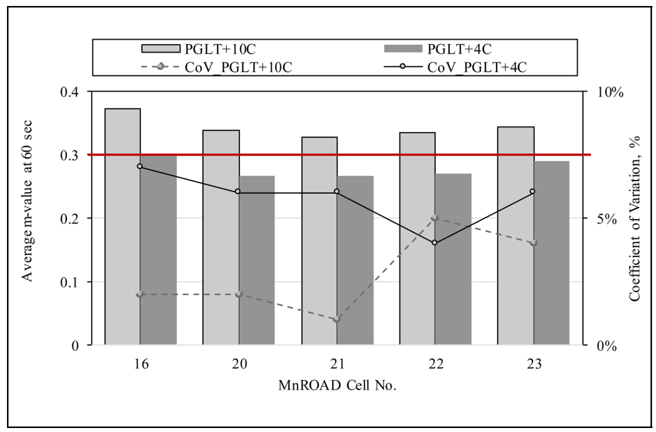

Figure 7. *M*-value at 60 s at PGLT + 10°C and PGLT + 4°C.

The results from the BBR strength test indicate that the binders have different failure properties. This is evident for the binder used in Cell 23 in particular; both the stress and strain at failure were significantly larger than the other binders of the same low temperature grade at PGLT + 10°C.

To further investigate differences in rheological and strength properties of binders, one-way analysis of variance (ANOVA) was performed. The significance level (α) was set at 0.05. The null hypothesis (H_0) assumed that all binder means were equal. The alternate hypothesis (H_a) was that at least one of the binder means was different. An example is given in Tables 3 and 4 that shows the ANOVA results for the PAV binder creep stiffness at 60 s at PGLT + 10°C.

The parameters in Table 4 are sum of squares (SS), degrees of freedom (df), mean square (MS), *F*-value, *P*-value, and *F*-critical. The degrees of freedom are obtained between groups (number of groups minus one) and within groups (number of total samples minus the number of groups). The sum of squares is calculated by adding the squared differences between the individual responses and the mean. The mean square is calculated by dividing the sum of squares by the degrees of freedom and the *F*-value is calculated as the ratio of between-groups mean square to within-groups mean square (*10*).

The *F*-value is greater than the *F*-critical value and the *P*-value is smaller than the alpha (α) level selected (0.05). It can be concluded that there is enough evidence to reject the null hypothesis and say that at least one of the five binders has significantly different means and belongs to a different population.

The analysis was also performed at PGLT + 4°C and the same approach was used for *m* (60 s), strength, and failure strain, for both test temperatures. The analyses indicate that for all combinations of properties and temperatures, there are significant differences among binders.

To identify these differences, an additional test was performed. Tukey's method, which is a pairwise comparison technique, was chosen because it provides simultaneous confidence intervals for differences of all pairs of means and controls the probability of making one or more Type I errors (*10*). The results of the pairwise comparison between binders are shown as boxplots in Figures 12 to 15. The boxplot provides a visual interpretation of the confidence intervals in which binders are grouped according to their means; binders with the same color and letter belong to the same group.

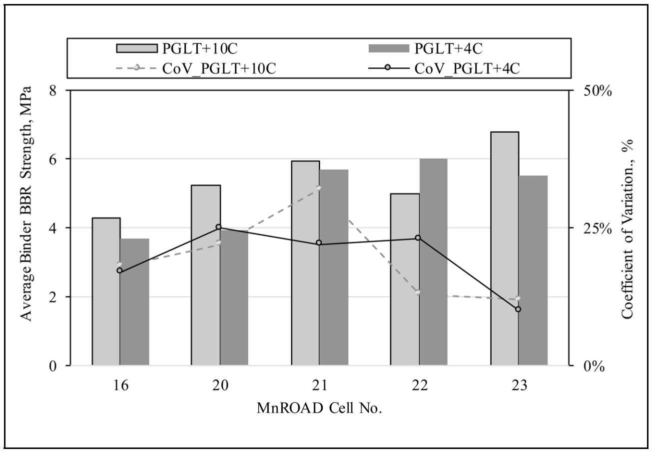

Figure 8. BBR strength at PGLT + 10°C and PGLT + 4°C.

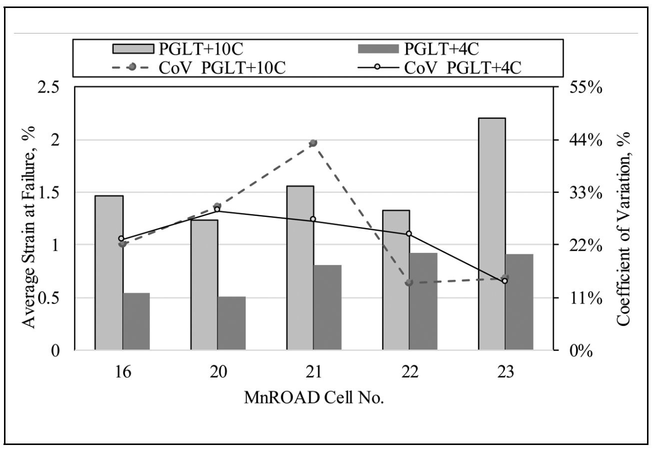

Figure 9. BBR failure strain at PGLT + 10°C and PGLT + 4°C.

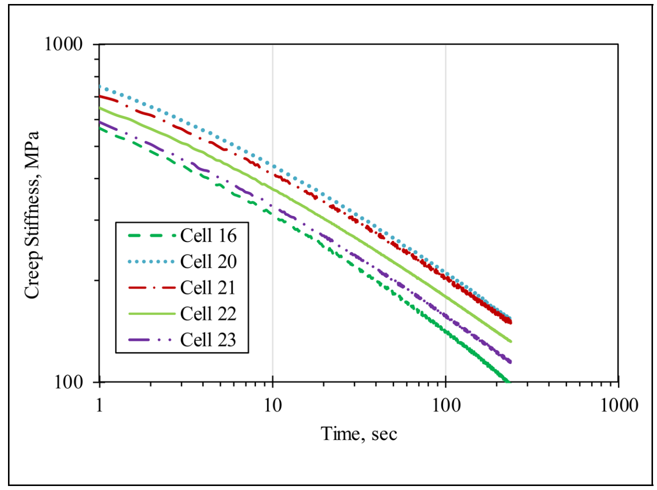

Figure 10. Creep stiffness vs. time at PGLT + 10°C.

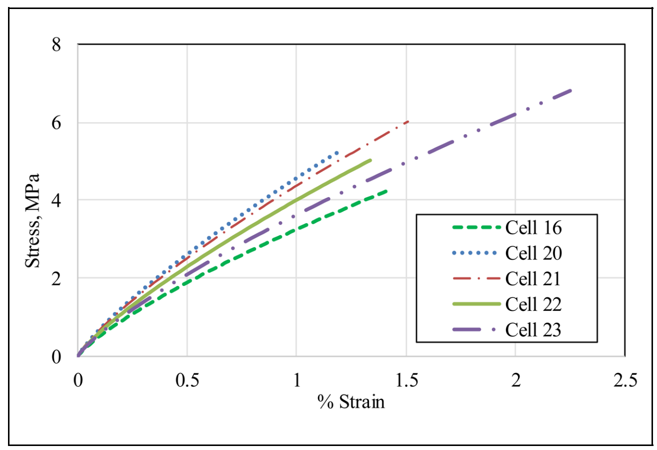

Figure 11. Stress–strain curves at PGLT + 10°C.

Several important observations can be made from the results presented in Figures 12 to 15. The grouping of binders based on similar rheological or strength characteristics changes with temperature. For example, in Figure 12, binders in Cells 16 and 23 belong to one group and binders from Cells 20, 21, and 22 belong to a different group, based on the creep stiffness at 60 seconds (S[60 s]) results at PGLT + 10°C. The grouping changes for PGLT + 4°C. From Figure 13, it is observed that the grouping based on m-value is different than the corresponding grouping based on S(60 s). It is interesting to note that binders in Cells 21 and 22 are placed in the same group based on stiffness and m-value, except for m-value at PGLT + 4°C. However, the two binders are grouped separately with respect to failure properties, except for BBR strength at PGLT + 10°C. As mentioned before, the binder in Cell 22 also contains an antistripping agent. The most visible difference is observed in Figures 14 and 15 in respect of the failure properties at PGLT + 10°C. In both figures, the binder in Cell 23 is grouped alone with the highest stress and strain at failure. The grouping changes at PGLT + 4°C; based on strength, Cell 21 and 23 binders are grouped together, and based on failure strain, Cell 22 and 23 binders are grouped together.

Conclusion

In this research, a simple testing protocol developed to obtain failure properties of asphalt binders at low temperatures was used to characterize the behavior of five asphalt binders at low temperature. The binders were used in 2016 to construct several test cells at MnROAD as part of a cracking experiment. Both creep and strength properties were obtained using a BBR-Pro at PGLT + 10°C and PGLT + 4°C, similar to current BBR and DTT specifications. After the beams were

Table 3. Summary: Single Factor for PAV Binder BBR Creep Stiffness at PGLT + 10°C

Groups	Count	Sum	Average	Variance
Cell 16	5	859.8016	171.9603	53.07403
Cell 20	4	1,006.217	251.5542	74.94623
Cell 21	5	1,203.323	240.6646	519.357
Cell 22	4	885.3054	221.3264	360.8912
Cell 23	5	948.5269	189.7054	65.00738

Table 4. ANOVA: Single Factor for PAV Binder BBR Creep Stiffness at PGLT + 10°C

Source of variation	SS	df	MS	*F*-value	*P*-value	*F*-critical
Between groups	21,183.38	4	5,295.845	24.71315	4.21E-07	2.927744
Within groups	3,857.266	18	214.2926	na	na	na
Total	25,040.65	22	na	na	na	na

Note: na = not applicable; SS = sum of squares; df = degrees of freedom; MS = mean square.

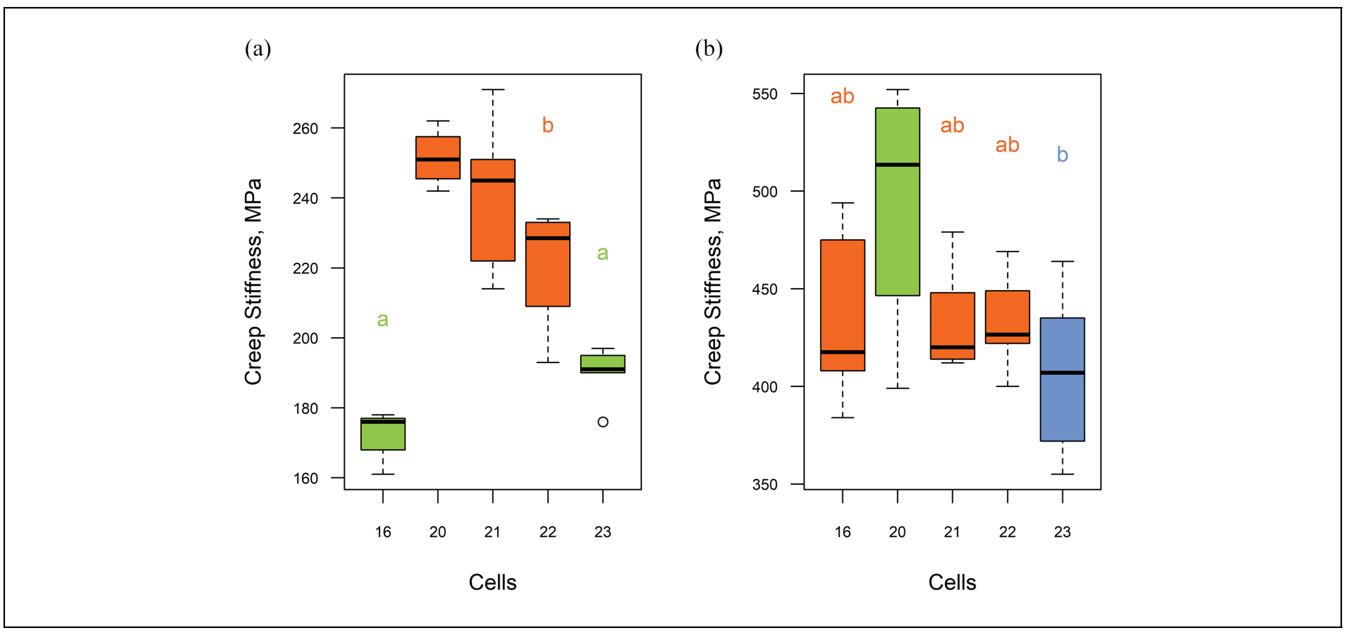

Figure 12. Boxplot for pairwise comparison for PAV Creep Stiffness at (*a*) PGLT + 10°C and (*b*) PGLT + 4°C.

conditioned at the test temperature for 1 h, a creep test was performed according to AASTHO T313. The beam was allowed to recover for 240 s after which a strength test was performed at a constant loading rate of 0.65 N/s. All binders were PAV aged and all testing was performed in air. Six replicates were tested for each binder and each temperature.

The results obtained indicate that the new protocol can be used to better discriminate between asphalt binders with similar rheological properties. Binders in Cells 20 to 23 have the same PGLT of −34, however, the failure properties are significantly different based on the statistical analyses performed. In particular, the asphalt binder used in Cell 23 has significantly higher failure

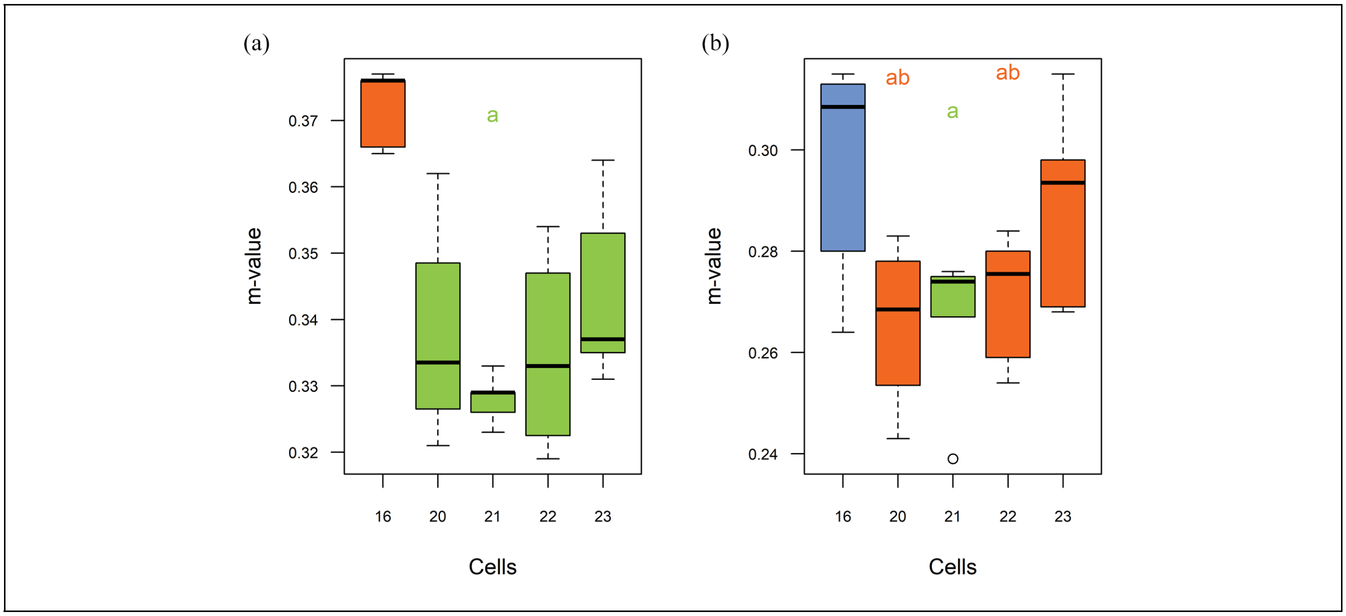

Figure 13. Boxplot for pairwise comparison for PAV *m*-value at (*a*) PGLT + 10°C and (*b*) PGLT + 4°C.

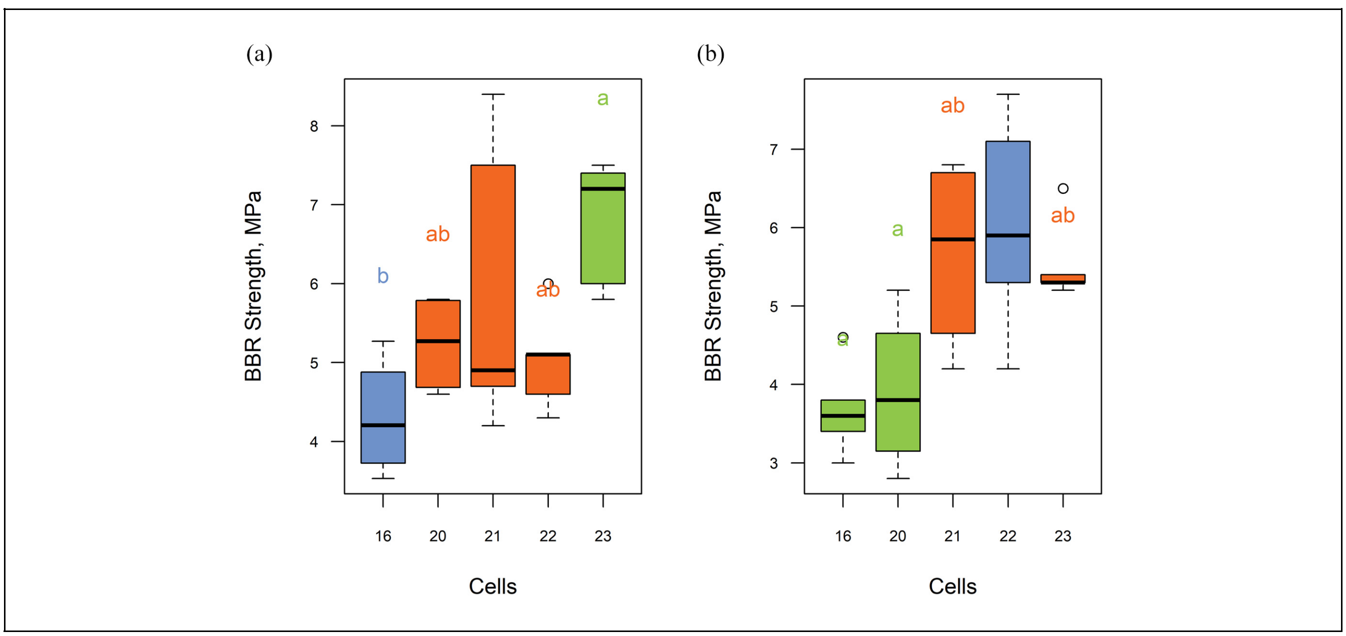

Figure 14. Boxplot for pairwise comparison for PAV BBR Strength at (*a*) PGLT + 10°C and (*b*) PGLT + 4°C.

stress and strain than the other binders. It was also noticed that the addition of antistripping agent may significantly change failure properties.

From a research point of view, it is clearly demonstrated that in the BBR strength test there are no deviations from the requirement of constant stress rate and that the BBR strength data is obtained under linear viscoelastic conditions for the entire duration of the test.

Based on the results of this investigation, it can be concluded that a combination of creep followed by strength testing provides a much better picture of the low temperature properties of asphalt binders and improves

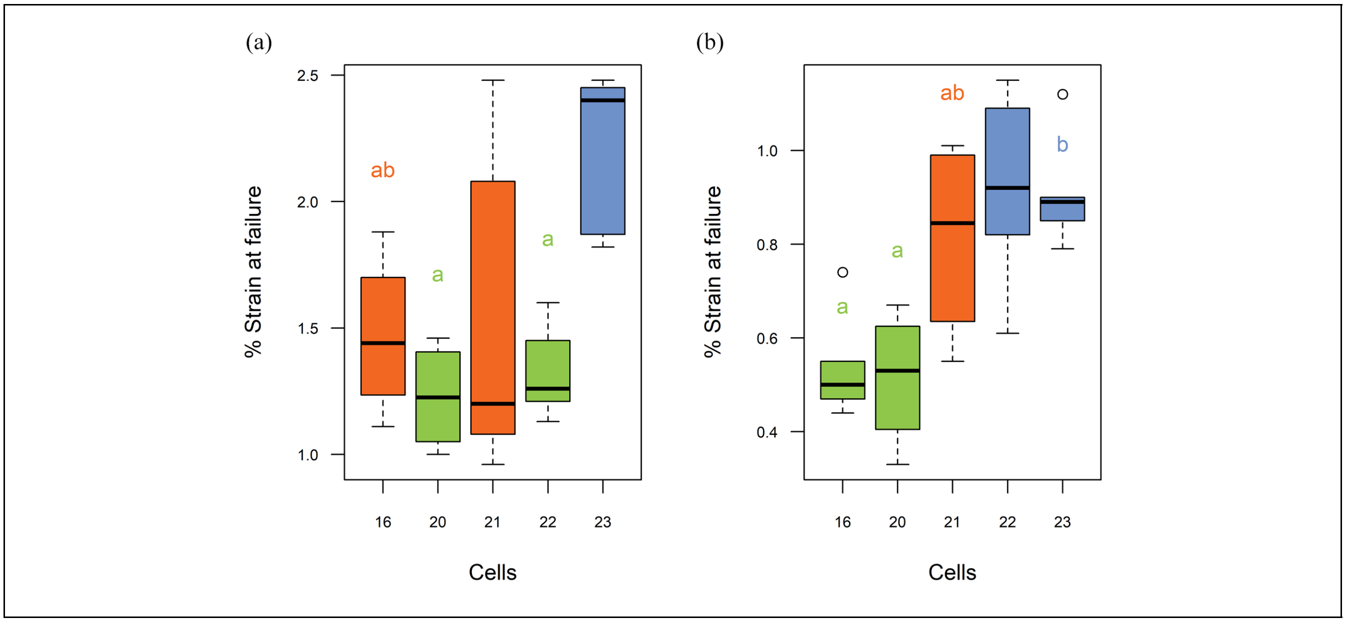

Figure 15. Boxplot for pairwise comparison for PAV BBR Strain at failure at (*a*) PGLT + 10°C and (*b*) PGLT + 4°C.

the selection process of asphalt binders for low temperature applications.

Acknowledgments

The financial and logistical support provided by Minnesota Department of Transportation is greatly acknowledged.

Author Contributions

The authors confirm contribution to the paper as follows: study conception and design: MM, DVD, DG; data collection: MT, DVD; analysis and interpretation of results: JMDO, TY, DG; draft manuscript preparation: MM, JMDO, TY. All authors reviewed the results and approved the final version of the manuscript.

References

1. Anderson, D. A., and T. W. Kennedy. Development of SHRP Binder Specification (With Discussion). *Journal of the Association of Asphalt Paving Technologists*, Vol. 62, 1993, pp. 481–507.
2. *Standard Method of Test for Determining the Flexural Creep Stiffness of Asphalt Binder Using the Bending Beam Rheometer (BBR)*. Specification T 313-12. AASHTO, Washington, D.C., 2012.
3. *Standard Method of Test for Determining the Fracture Properties of Asphalt Binder in Direct Tension (DT)*. Specification T 314-12. AASHTO, Washington D.C., 2012.
4. Dongré, R. *Development of Direct Tension Test Method to Characterize Failure Properties of Asphalt Cements*. Pennsylvania State University, State College, 1994.
5. Marasteanu, M. O., and D. A. Anderson. Comparison of Moduli for Asphalt Binders Obtained from Different Test Devices. *Journal of the Association of Asphalt Paving Technologists*, Vol. 69, 2000, pp. 574–607.
6. Marasteanu, M. O., A. C. Falchetto, M. Turos, and J. L. Le. *Development of a Simple Test to Determine the Low Temperature Strength of Asphalt Mixtures and Binders*. IDEA Program Final Report, NCHRP-151. Transportation Research Board of the National Academies, Washington, D.C., 2012.
7. Falchetto, A. C., M. I. Turos, and M. O. Marasteanu. Investigation on Asphalt Binder Strength at Low Temperatures. *Road Materials and Pavement Design*, Vol. 13, No. 4, 2012, pp. 804–816.
8. Marasteanu, M., D. Ghosh, A. C. Falchetto, and M. Turos. Testing Protocol to Obtain Failure Properties of Asphalt Binders at Low Temperature Using Creep Compliance and Stress-Controlled Strength Test. *Road Materials and Pavement Design*, Vol. 18, 2017, pp. 1–16.
9. Ferry, J. D. *Viscoelastic Properties of Polymers*, 3rd ed. Wiley & Sons, New York, 1980.
10. Oehlert, G. W. *A First Course in Design and Analysis of Experiments*. W. H. Freeman, New York, 2000.

The Standing Committee on Asphalt Binders (AFK20) peer-reviewed this paper (19-05954).

The results and opinions presented do not necessarily reflect those of the sponsoring agencies.